THE JOURNAL OF BIOLOGICAL CHEMISTRY VOL. 285, NO. 43, pp. 33242–33251, October 22, 2010

p38 MAP Kinase and MAPKAP Kinases MK2/3 Cooperatively Phosphorylate Epithelial Keratins*[S]

Received for publication, April 9, 2010, and in revised form, August 13, 2010 Published, JBC Papers in Press, August 19, 2010, DOI 10.1074/jbc.M110.132357

Manoj B. Menon[‡], Jessica Schwermann[‡], Anurag Kumar Singh[§], Mirita Franz-Wachtel[¶], Oliver Pabst[‖], Ursula Seidler[§], M. Bishr Omary[**], Alexey Kotlyarov[‡], and Matthias Gaestel[‡1]

From the [‡]Institute of Biochemistry, [§]Department of Gastroenterology, Hepatology, and Endocrinology, and [‖]Institute of Immunology, Medical School Hannover, Hannover 30625, Germany, the [¶]Proteome Center Tübingen, Interfaculty Institute for Cell Biology, University of Tübingen, Tübingen 72076, Germany, and the [**]Department of Molecular and Integrative Physiology, University of Michigan, Ann Arbor, Michigan 48109

The MAPK-activated protein kinases (MAPKAP kinases) MK2 and MK3 are directly activated via p38 MAPK phosphorylation, stabilize p38 by complex formation, and contribute to the stress response. The list of substrates of MK2/3 is increasing steadily. We applied a phosphoproteomics approach to compare protein phosphorylation in MK2/3-deficient cells rescued or not by ectopic expression of MK2. In addition to differences in phosphorylation of the known substrates of MK2, HSPB1 and Bag-2, we identified strong differences in phosphorylation of keratin 8 (K8). The phosphorylation of K8-Ser^{73} is catalyzed directly by p38, which in turn shows MK2-dependent expression. Notably, analysis of small molecule p38 inhibitors on K8-Ser^{73} phosphorylation also demonstrated reduced phosphorylations of keratins K18-Ser^{52} and K20-Ser^{13} but not of K8-Ser^{431} or K18-Ser^{33}. Interestingly, K18-Ser^{52} and K20-Ser^{13} are not directly phosphorylated by p38 *in vitro*, but by MK2. Furthermore, anisomycin-stimulated phosphorylations of K20-Ser^{13} and K18-Ser^{52} are inhibited by small molecule inhibitors of both p38 and MK2. MK2 knockdown in HT29 cells leads to reduced K20-Ser^{13} phosphorylation, which further supports the notion that MK2 is responsible for K20 phosphorylation *in vivo*. Physiologic relevance of these findings was confirmed by differences of K20-Ser^{13} phosphorylation between the ileum of wild-type and MK2/3-deficient mice and by demonstrating p38- and MK2-dependent mucin secretion of HT29 cells. Therefore, MK2 and p38 MAPK function in concert to phosphorylate K8, K18, and K20 in intestinal epithelia.

Intermediate filaments are important structural and functional components of eukaryotic cells. Together with the microfilament and microtubule network they constitute the third major filament system of the cytoskeleton, characterized by their unique expression patterns and nonpolar filament association. Keratins (K)[2] are cytoplasmic intermediate filaments preferentially expressed in the epithelium. The 54 keratin genes in human genome can be divided into type I (acidic) and type II (basic) keratins. They exist as obligate noncovalent heteropolymers consisting of at least one type I (K9–K28, K31–40) and one type II keratin (K1–K8, K71–86) in an equimolar ratio (1). The keratins of the single layered epithelium mainly express K8 and K18 and, depending on the cell type, variable amounts of K7, K19, and K20 (2). For example, hepatocytes exclusively express K8/18, whereas intestinal epithelial cells express K8/18/19/20. Several post-translational modifications are known to modulate the keratin filaments. Phosphorylation is by far the most studied modification of keratins, and phosphorylation sites were identified in all major keratins of the single-layered epithelium (K8/18/19/20) (3).

The p38 MAPK (p38) pathway is activated by proinflammatory cytokines, radiation, and osmotic and chemical stress (4). p38 has been implicated as the physiological protein kinase responsible for K8 phosphorylation during mitosis and under various cellular stress stimuli (5). Pharmacological inhibition of p38 using SB202190 was shown to be sufficient to block orthovanadate-induced keratin filament breakdown completely (6). K8-Ser^{73} phosphorylation by p38 was associated with, but not sufficient for keratin filament destabilization. This suggested involvement of additional p38-dependent keratin phosphorylation sites.

MAPK-activating protein (MAPKAP) kinases 2 (MK2) and 3 (MK3) are well characterized downstream targets of p38, with MK2 having predominant physiological relevance due to its higher abundance compared with MK3 (7). Two distinct roles for MK2 in the cellular stress response involve cytokine biosynthesis and cytoskeleton modulation. MK2/3 are shown to phosphorylate several actin-modulating proteins including HSPB1, which greatly explains the reduced migratory phenotype of MK2/3- and p38-deficient cells (8–10). Vimentin, a member of the intermediate filament family, was shown to be a MK2 substrate (11), whereas no role for MK2 is known in keratin phosphorylation so far. Early studies on okadaic acid-induced hyperphosphorylation of keratins suggested the role of a stau-

* This work was supported, in whole or in part, by National Institutes of Health Grant DK47918 (to M. B. O.). This work was also supported by the Deutsche Forschungsgemeinschaft (M. G.), Deutsche Forschungsgemeinschaft Grant Se 460/13-4 (to U. S.). The Proteome Centrum Tübingen is supported by the Ministerium für Wissenschaft und Kunst, Landesregierung Baden-Württemberg.

[S] The on-line version of this article (available at http://www.jbc.org) contains supplemental Figs. 1–3.

[1] To whom correspondence should be addressed: Medical School Hannover, Institute of Biochemistry, Carl-Neuberg-Str. 1, D-30625 Hannover, Germany. Tel.: 49 511 532 2825; Fax: 49 511 532 2849; E-mail: gaestel.matthias@mh-hannover.de.

[2] The abbreviations used are: K, keratin; DKO, double knock-out; ELLA, enzyme-linked lectin assay; MK (MAPKAPK), MAPK-activated protein kinase; MEF, mouse embryonic fibroblast; PGE2, prostaglandin E2.

rosporine-sensitive serine/threonine kinase whose activity is controlled by protein phosphatases 1/2A (12). MK2 is strongly activated by okadaic acid (11) and is sensitive to staurosporine and could be a perfect candidate for stress-induced keratin phosphorylation. Apart from its role in substrate modification, MK2/3 binds to p38 and stabilizes it. Hence, in the absence of MK2/3, reduced levels of p38 protein and activity are detected (9, 13).

In search for novel substrates of MK2/3 we conducted a two-dimensional PAGE-based proteomics study, which showed reduced expression and phosphorylation of K8 in MK2/3-deficient cells. Further analysis of p38/MK2 dependence on phosphorylation of the epithelial keratins K8/18/20 revealed a role for MK2 in phosphorylation of K18 and K20. For the first time we show functional cooperation of p38 and MK2/3 in signaling to keratins and prove conclusively that MK2/3 are responsible for K20 phosphorylation *in vivo*.

MATERIALS AND METHODS

Antibodies and Reagents—p38 MAPK, phospho-p38 MAPK, MAPKAPK-2, and phospho-MAPKAPK-2 (Thr^{222}) antibodies were from Cell Signaling Technology, Inc. Anti-phospho-HSPB1 (mouse-Ser^{86}/human-Ser^{82}) antibody was from Invitrogen, anti-GAPDH antibody from Chemicon International, anti-murine HSPB1 (mHSPB1) antibody from Stressgen, and anti-human HSPB1 (hHSPB1) antibody from Santa Cruz Biotechnology. Antibodies used against phosphokeratins were LJ4 (K8-$Ser(P)^{73}$ (14)), 5B3 (K8-$Ser(P)^{431}$ (15)), Ab3055 (K18-$Ser(P)^{52}$ (16)), Ab8250 (K18-$Ser(P)^{33}$ (17)), and Ab2667 (K20-$Ser(P)^{13}$ (18)). Total keratin antibodies used were Ks20.8 (K20; Neomarkers), Ab4668 (K18) (19), and L2A1 (K8/18) (20). All peroxidase-labeled secondary antibodies were from Santa Cruz Biotechnology, and fluorescent labeled antibodies were from Molecular Probes. Anisomycin and SB203580 were purchased from Calbiochem, SB202190 and BIRB-796 were from Axon Ligands. The MK2/3/5 inhibitor PHA-781089 was provided by Pfizer. K8/18 proteins and anti-K8 antibody were provided by Dr. Harald Herrmann. Recombinant human K20 was purchased from Progen. Lentiviral shRNA transduction particles were from Sigma (Mission shRNA). 16,16-Dimethyl-PGE2 was obtained from Sigma.

Mice—MK2/3-double deficient mice were obtained as described earlier (13). Mice were bred and maintained under specific pathogen-free conditions in the central animal facility at Hannover Medical School.

Cell Culture and Treatment—MK2/3-deficient immortalized MEFs rescued with MK2, MK2-K79R (previously reported as K76R), or control vector by retroviral transduction were generated and maintained as reported earlier (10, 13). HT29 cells were maintained in DMEM/F12 (1:1) containing 10% serum, 2.5 mM L-glutamine, 100 units of penicillin G/ml, and 100 μg of streptomycin/ml. HT29-MTX cells (21) were maintained in DMEM/10%FCS with 4 mM L-glutamine. For Western blots, cells were seeded in 6-well plates and stimulated with the indicated concentrations of anisomycin for 30 min. All inhibitors were added 1 h prior to anisomycin treatment. MEFs were transfected in 6-well plates with 5 μg of total plasmid DNA by Lipofectamine Plus reagent (Invitrogen) following the manufacturer's protocol.

Proteomic Analysis—MK2/3-double deficient immortalized MEFs transduced with empty vector or retroviral vector encoding MK2 were stimulated with anisomycin. Two-dimensional PAGE analysis of the cell lysates was done according to Barjaktarović *et al.* (22) with the following modifications: 250 μg protein of each sample was used, dissolved in rehydration buffer (8 M urea, 2 M thiourea, 4% CHAPS, 1% DTT, 0.7% Pharmalytes pH 3–10, and 0.001% bromphenol blue) supplemented with Complete™ protease inhibitor mixture (Roche Applied Science) and phosphatase inhibitor mixture I (Sigma-Aldrich) were separated on immobilized 24-cm pH gradient polyacrylamide gel strips in the pH range of 3–10. After rehydration the voltage was progressively increased to 10,000 V. Isoelectric focusing was stopped after 65 kVh was reached. For the second dimension the equilibrated gel strips were applied to 12% polyacrylamide gels. To detect phosphorylated proteins, gels were first stained with Pro-Q Diamond (Invitrogen) followed by silver staining for total protein detection. Concerning each state, protein preparations from two independent experiments were subjected to two-dimensional PAGE meaning two biological replicates, respectively. Gels were comparatively analyzed using the software Delta2D (version 3.4; Decodon, Greifswald, Germany). Spot evaluation, protein digestion, and analysis by electrospray ionization-tandem MS were done as described elsewhere (21).

Generation of MK2 Knock-down Cells—To knock down MK2 expression, HT29 cells were transduced with the SHVRS MISSION shRNA lentiviral particles (Sigma). Five different lentiviral particles were used (catalogue no. TRCN2282–6) together with the control lentiviral particles (MISSION non-target shRNA control). The cells were transduced in 96-well plates at a multiplicity of infection of 2 and 3. After transduction, cells were selected with puromycin (2 μg/ml), and MK2 expression was analyzed by Western blotting. Four cell lines showing the best knockdown were analyzed for substrate phosphorylation.

Western Blotting—Cells were harvested, washed, and boiled in SDS loading buffer. For blotting intestinal tissue, mice were killed and small intestine removed. After thoroughly flushing with PBS, the ileum was cut open, minced, and boiled in 2× SDS loading buffer. Soluble protein extract was run on SDS-PAGE (7.5–16% gradient) gels and transferred to Hybond ECL membranes (Amersham Biosciences). Blots were incubated for 1 h in PBS-0.1% Tween 20 containing 5% powdered skim milk. After three washes with PBS-0.1% Tween 20, membranes were incubated for 16 h with the primary antibody at 4 °C and for 1 h with horseradish peroxidase-conjugated secondary antibodies at room temperature. Blots were developed with an ECL detection kit (Santa Cruz Biotechnology), and the digital chemiluminescence images were taken by a Luminescent Image Analyzer LAS-3000 (Fujifilm). Bands were quantified using TINA software (RayTest).

In Vitro Kinase Assays—*In vitro* kinase assays were performed as described previously (23). In the case of radioactive kinase assay, ^{33}P-labeled phosphoproteins were detected by the BioImaging Analyzer BAS 2000 (Fuji). For site-specific assays,

TABLE 1

Proteins that are less phosphorylated in MK2/3-double deficient MEFs are evaluated by two-dimensional PAGE and identified by electrospray ionization-tandem MS

Protein ID	Protein name	Molecular mass[a]	pI[b]	Sequence coverage[c]	Mascot score[d]
		kDa		%	
AAI06155	Keratin 8 (*Mus musculus*)	54.51	5.7	35	1,111
AAA18336	Heat shock protein HSPB1 (*Mus musculus*)	21.96	6.45	10	91
NP_663367	Bcl2-associated athanogene 2 (*Mus musculus*)	23.45	6.01	12	157

[a] Molecular mass of predicted proteins.
[b] pI value of predicted proteins.
[c] Percentage of predicted protein sequence covered by matched peptides.
[d] Probability-based MOWSE score.

nonradiolabeled ATP was used, and the reactions after gel separation were probed using phospho-specific antibodies.

Fluorescence Microscopy—For microscopy, HT29 cells were seeded on poly-L-lysine-coated coverslips. After treatments, cell layers were washed three times and fixed with cold (−20 °C) methanol for 10 min. Samples were blocked with 3% BSA-PBS for 1 h followed by a 2-h incubation in primary antibodies diluted in 1.5% BSA-PBS. After three PBS washes, secondary antibodies (Alexa Fluor 488/Alexa Fluor 546) were added and incubated for 1 h. After three washes coverslips were mounted and analyzed using a Leica DM IRBE microscope (40× oil immersion objective) with the Leica TCS confocal systems program.

For immunohistochemistry of mouse ileum, isolated small intestines were processed as described previously (13) and stained with K20-Ser(P)[13] antibody. Nuclei were stained with DAPI. Fluorescence images were taken using an IX81 microscope and analySIS D software (Olympus).

In Vitro Mucin Secretion Studies—HT29-MTX cells (21) were seeded in 12-well plates at a density of 24,000 cells/cm^2 and cultured for 14 days, serum-starved for 24 h prior to the experiment, and stimulated with 16,16 dimethyl-PGE2 in 1 ml of serum-free medium for 30 min. Wherever indicated, inhibitors were added 30 min prior to stimulation. Supernatants were collected after thorough mixing and centrifuged at 8,000 × *g* for 10 min. Dilutions of cleared supernatants were used for enzyme-linked lectin assay (ELLA).

In Vivo Mucin Secretion Studies—For ileal mucin sampling, an *in vivo* ileal loop experiment was performed exactly as previously described for duodenal and jejunal loop (24), except that the mice were anesthetized by isoflurane (Forene®; Abbott) inhalation. Approximately 5 cm of intestine was perfused at the rate of 15 ml h^{-1} with 154 mM NaCl. After the surgery, mice were left to recover for 30 min, for washout of intestinal contents and fluid resuscitation after surgical trauma. After the recovery period, the basal mucin secretion was monitored for 20 min at 5-min intervals. 5 μM 16,16 dimethyl-PGE2 was perfused for 30 min and samples collected at every 5 min. Samples were diluted 20–600 times and analyzed by ELLA. Mucin secreted per centimeter of ileum length per h (μg/cm per h) was calculated for each sample. The data were presented as percentage secretion by taking total mucin secreted in the basal and stimulated state together as 100%, to avoid variations due to differences in stored mucin content between different animals.

ELLA—ELLA for measuring mucin-like glycoprotein secretion was modified from a previously published method (25). Briefly, wells of a 96-well plate were coated with 100 μl of standards or with sample dilutions in sodium carbonate buffer (0.1 M, pH 9.6) and then incubated overnight at 4 °C. The following day, the microplate was washed and blocked with 3% BSA in PBST for 60 min at 37 °C. The wells were incubated with 100 μl of biotinylated wheat germ agglutinin (2 μg/ml) (Galab Technologies) in PBST and 1.5% BSA for 60 min at 37 °C. After washes, 100 μl of streptavidin-peroxidase conjugate (Invitrogen) was added and allowed to bind for 60 min at room temperature. After washing, 100 μl of TMB substrate solution (Sigma)

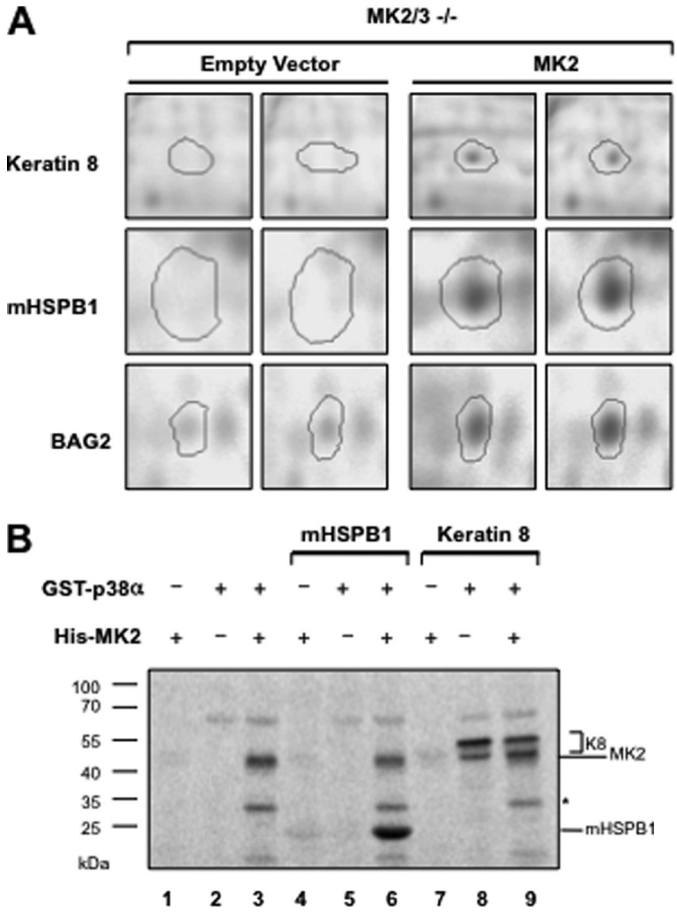

FIGURE 1. **Reduced K8 phosphorylation in MK2/3-double deficient MEFs.** *A*, MK2/3-deficient cells stably transduced with empty vector and MK2 expression vector in duplicates were stimulated with 10 μg/ml anisomycin for 30 min. Cell lysates were analyzed by two-dimensional PAGE and stained with Pro-Q Diamond phosphoprotein gel stain. The spots for K8, mHSPB1, and BAG2 with reduced staining in the gels of MK2/3-deficient cell lysates are shown. *B*, K8 and mHSPB1 were subjected in parallel to *in vitro* radioactive kinase assays with purified His-MK2 (*lanes 4* and *7*), GST-p38 (*lanes 5* and *8*), or with both (*lanes 6* and *9*). Reactions were separated on 7.5–22.5% gradient SDS-PAGE and analyzed by phosphorimaging.

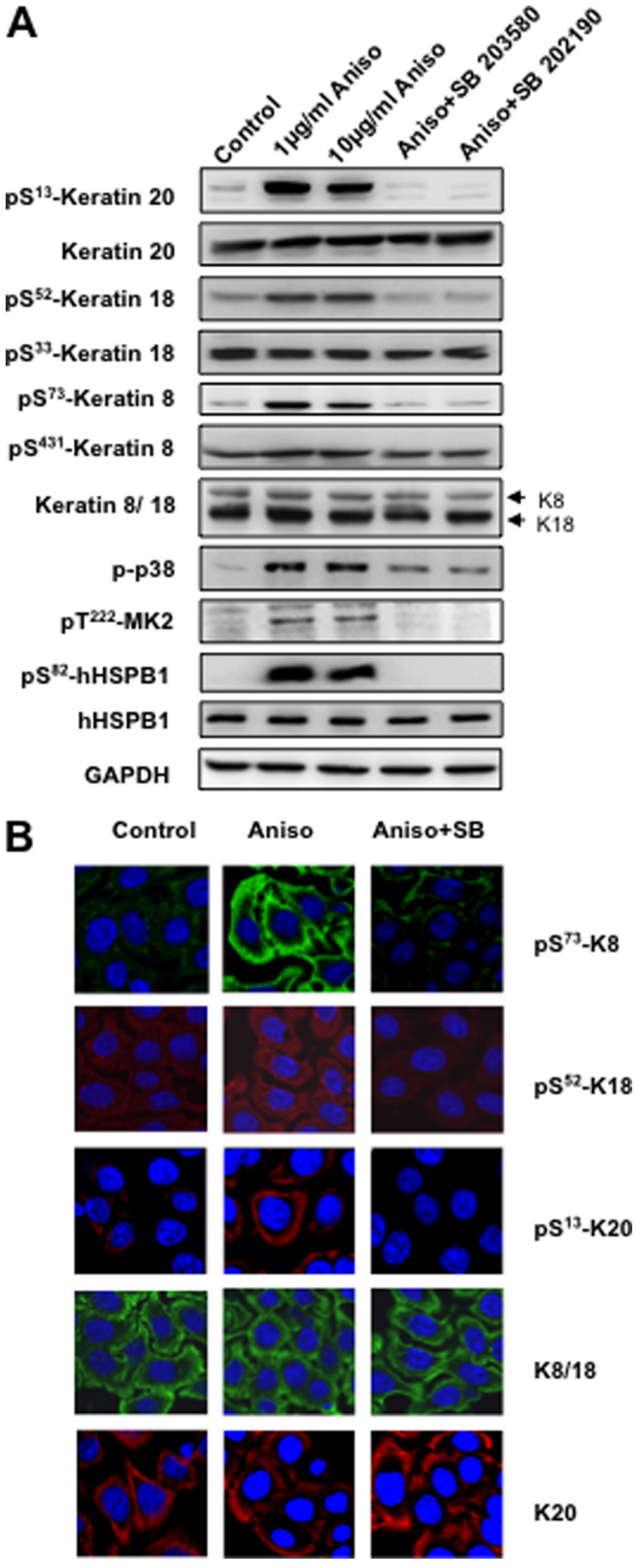

FIGURE 2. **Stress-induced keratin 8/18/20 phosphorylation is p38-dependent.** *A*, HT29 cells were stimulated with 1 or 10 μg/ml anisomycin (*Aniso*) for 30 min. For p38 inhibition, cells were pretreated with 5 μM SB203580/5 μM SB202190 for 1 h followed by a 30-min stimulation with 10 μg/ml anisomycin. After treatment, the samples were analyzed by Western blotting using antibodies to the indicated antigens. GAPDH was used as a loading control. *B*, HT29 cells grown on coverslips were left untreated or stimulated for 30 min with anisomycin, with or without pretreatment with 5 μM SB202190. Cells were fixed and stained using antibodies to the indicated antigens.

was added to each well. The reaction was stopped by adding 50 μl of 0.5 M sulfuric acid to each well. The absorbance was read at 450 nm and 630 nm as reference. Crude size-fractionated mucin-like glycoprotein isolated from HT29-MTX supernatant was used as standard.

RESULTS

MK2/3-deficient Cells Show Reduced K8 Phosphorylation—A proteomics study undertaken to identify novel substrates of MK2/3 showed reduced phosphorylation of K8 in MK2/3-double deficient MEFs compared with MK2/3-deficient cells rescued by MK2 expression (Table 1 and Fig. 1*A*). Because this experiment also documented differential phosphorylation of known substrates of MK2 (Bag2 and HSPB1) and because no overall differences in the Pro-Q Diamond phosphoprotein staining intensity between both gels were seen (*cf.* supplemental Fig. 1), the finding was regarded relevant and p38/MK2-dependent K8 phosphorylation was analyzed further. *In vitro* kinase assay showed that p38, but not MK2, could directly phosphorylate human K8 (Fig. 1*B*). As assay controls, mHSPB1 is shown as a bona fide substrate of MK2 and MK2 as a substrate of p38. MK2/3-deficient cells were previously shown to display a reduced level of p38 (13) because MK2/3 are necessary for p38 stability. Thus, the reduced K8 phosphorylation in MK2/3-deficient cells could be attributed to the reduced amount and activity of p38 in the absence of MK2/3.

Stress-induced Phosphorylation of K8/18 and K20 Is p38 MAPK-dependent—Because keratins were shown to be phosphorylated in response to stress stimuli, we looked at the role of p38 in phosphorylation of other epithelial keratins in HT29 cells, human intestinal epithelial cells of colon adenocarcinoma origin (Fig. 2*A*). Of the two major MAPK-dependent phosphorylation sites in K8, Ser^{73} phosphorylation takes place via p38 kinase (5) and c-Jun N-terminal kinase (26) in a context-dependent manner. Consistent with these published data, phosphorylation at K8-Ser^{73} was abolished by the p38 inhibitors (SB202190, SB203580), and the Ser^{431} site, which was earlier shown to become phosphorylated by ERK1/2 (15), was neither activated by the p38-specific stimuli nor blocked by p38 inhibitors. Interestingly, we could detect strong anisomycin-induced phosphorylation of K18-Ser^{52} and K20-Ser^{13} that was completely abrogated by p38 MAPK inhibitors (Fig. 2*A*). In contrast, K18-Ser^{33}, another known phosphorylation site, showed neither anisomycin-induced phosphorylation nor an effect of p38 inhibition. The stress- and p38-dependent phosphorylation of K8, K18, and K20 was confirmed by immunostaining of HT29 cells (Fig. 2*B*). Here, anisomycin treatment clearly enhances the staining by phospho-specific antibodies, whereas the staining for total keratins is not affected. SB202190 pretreatment drastically down-regulates the phosphokeratin staining.

p38 Directly Phosphorylates K8, whereas MK2 Directly Phosphorylates K18 and K20 in Vitro—The above inhibitor studies confirmed the role of p38 pathway in K8/18/20 phosphoryla-

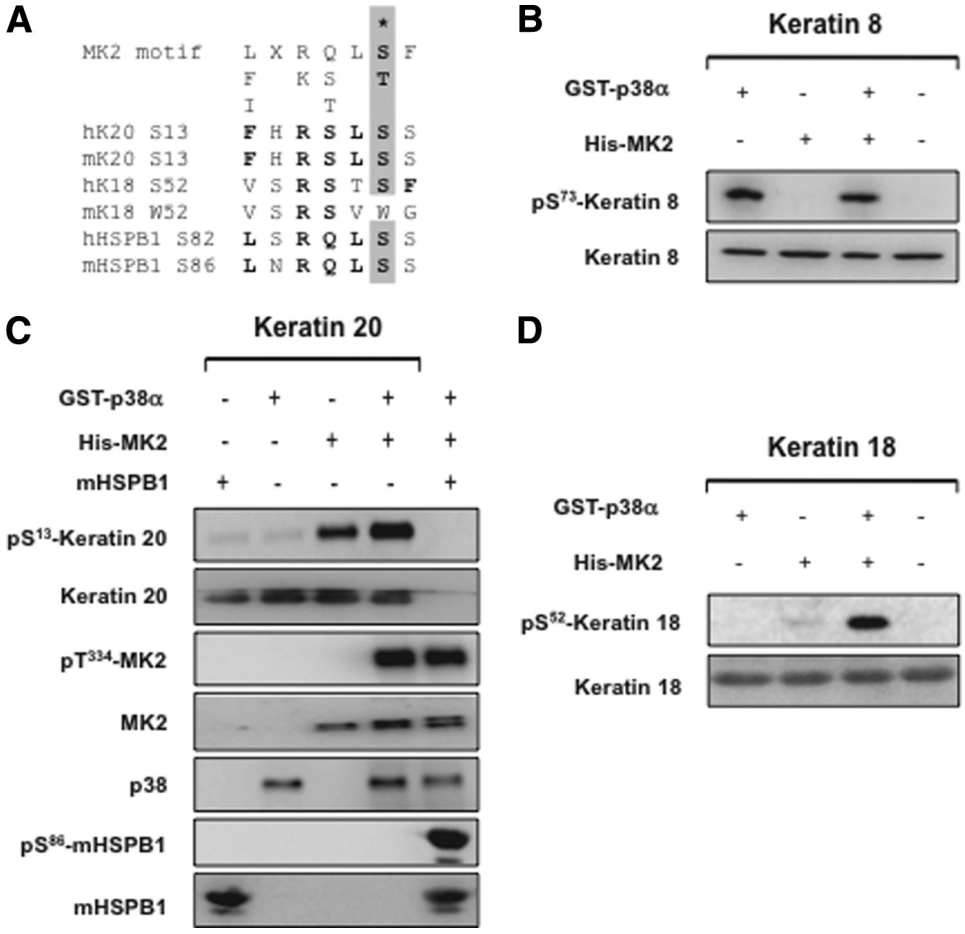

FIGURE 3. **MK2 directly phosphorylates K18 and K20 *in vitro*.** *A*, comparison of phosphorylation sites in K18/20 with that of MK2 substrates mHSPB1/hHSPB1 and consensus MK2/3 phosphorylation site. Matching residues are in *bold*, and the phosphorylated S/T is denoted. *B*, *in vitro* kinase assay with GST-p38/His-MK2 followed by Western blotting for K8-Ser^{73} phosphorylation and for total K8 protein. *C*, *in vitro* kinase assay for K20-Ser^{13} phosphorylation. mHSPB1-Ser^{86} and MK2-Thr^{334} phosphorylations are shown as controls. *D*, *in vitro* kinase assay for K18-Ser^{52} phosphorylation.

tion. However, p38 phosphorylates its substrates in a proline-directed manner (4). Although the K8-Ser^{73} site is situated within such a motif conserved in a number of type II cytokeratins (27), the phosphorylated residues in K18 and K20 are not proline-directed but located within a perfect consensus motif for direct MK2/3-mediated phosphorylation (7) (Fig. 3*A*). *In vitro* kinase assay followed by Western blot analysis confirmed that p38 directly phosphorylates K8 at Ser^{73}, independent of MK2 (Fig. 3*B*). Interestingly, MK2 but not p38 phosphorylates K18-Ser^{52} and K20-Ser^{13} (Fig. 3, *C* and *D*). HSPB1, a bona fide substrate of MK2, was used as a positive control for the *in vitro* kinase assays. As described earlier, recombinant MK2 shows very low enzymatic activity (23) which could be significantly enhanced by p38 MAPK-mediated phosphorylation and activation. p38 MAPK-mediated phosphorylation of MK2 at Thr^{334} is shown as a control.

Restoration of p38 Levels Rescues K8-Ser^{73} Phosphorylation in MK2/3 Double Knock-out (DKO) MEFs—Because K8-Ser^{73} phosphorylation was found to be stress-activated and a direct target of p38, we analyzed K8-Ser^{73} phosphorylation in MK2/3-deficient cells. Because the levels of K8/18 in MEFs were not sufficient to be detected by immunoblotting, we analyzed cells with transfected K8/18. Previous studies have shown that the reduced p38 levels in MK2/3 DKO cells could be rescued by a catalytically inactive mutant of MK2 (MK2-K79R) (9, 13). When K8-Ser^{73} phosphorylation was monitored in MK2/3 DKO cells transduced with MK2 or MK2-K79R, there was comparable rescue of phosphorylation. The overexpressed K8 was phosphorylated independent of anisomycin stimulation and was sensitive to SB202190 (Fig. 4). This conclusively proves that reduced K8 phosphorylation in MK2/3-deficient cells is an effect of reduced p38 levels and activity and is not caused by the loss of catalytic activity of MK2/3. Furthermore and consistent with the *in vitro* data, K18-Ser^{52} phosphorylation was dependent on MK2 catalytic activity and could not be rescued by MK2-K79R. Phosphorylation of HSPB1, a bona fide substrate of MK2, and MSK1, a p38 MAPK substrate, are shown as controls.

Pharmacological Inhibition of MK2/3 Blocks K18 and K20 Phosphorylation—To confirm further the role of MK2/3 in phosphorylation of K20, we analyzed the effect of MK2/3/5 inhibitor PHA-781089 on stress-induced K20 phosphorylation in HT29 cells. PHA-781089 dose dependently down-regulated K20-Ser^{13} phosphorylation as well as mHSPB1-Ser^{82} phosphorylation (Fig. 5*A*). p38 inhibitors SB202190 and BIRB-796 were used as positive controls. Consistent with the previous results, K18-Ser^{52} showed the same pattern of inhibition, whereas K8-Ser^{73} was affected only by p38 inhibitors. Because Ser^{13} is evolutionarily conserved and present in both mouse and human K20, whereas Ser^{52} is only present in human K18 and not conserved in mouse K18 (*cf.* Fig. 3*A*), we focused on K20 phosphorylation in further experiments in more detail. Immunostaining of HT29 cells, with phosphorylation-specific and pan-K20 antibodies, reconfirmed the effect of MK2 and p38 inhibitors on anisomycin-stimulated K20-Ser^{13} phosphorylation (Fig. 5*B*).

Specific Knockdown of MK2 in HT29 Cells Down-regulated K20 Phosphorylation—In murine cells, MK2 has been shown to have a dominant role in MK2/MK3 signaling due to its higher level of expression compared with MK3 (13). Direct comparison of active MK2 and MK3 in HT29 cells indicated that they express very low levels of MK3 (data not shown). Hence, we expected effects on K20-Ser^{13} phosphorylation by stable knockdown of MK2 even in the presence of MK3 in these cells. Indeed, MK2 knockdown showed the same effect on K20 phos-

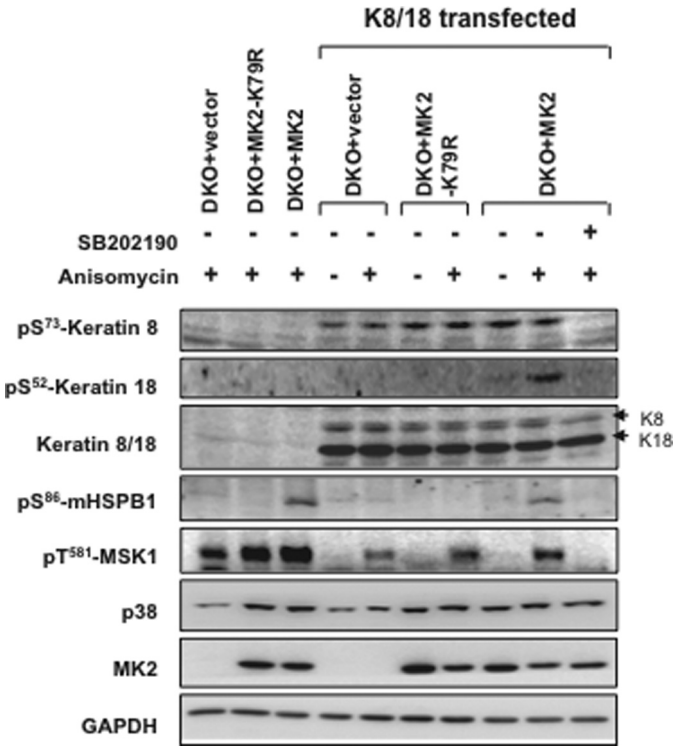

FIGURE 4. **Catalytically inactive MK2 rescues K8-Ser^{73} phosphorylation in MK2/3 DKO cells.** MK2/3-deficient cells transduced retrovirally with MK2, MK2-K79R, or empty vector (GFP) were transfected with plasmids expressing human K8 and K18 or control vector. 24 h after transfection, cells were serum-starved for 10 h. Wherever indicated, cells were stimulated for 30 min with 10 μg/ml anisomycin. SB202190 (5 μM) pretreatment was given for 60 min where indicated. K8-Ser^{73} and K18-Ser^{52} were analyzed by Western blotting. Rescue of p38 levels by MK2 or MK2-K79R is shown. Phospho-MSK-Thr^{581}, HSPB1-Ser^{86}, total K8/18, GAPDH, and MK2 were probed as controls.

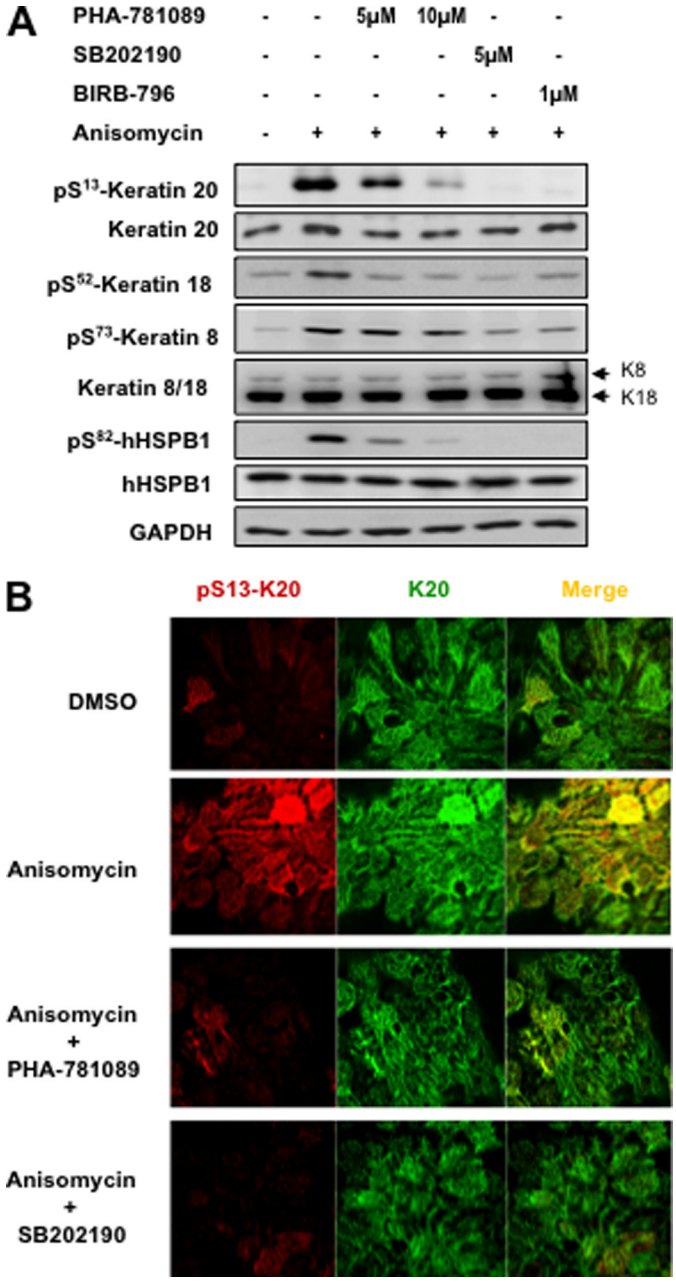

FIGURE 5. **MK2/3/5 inhibitor inhibits stress-induced K18/20 phosphorylation.** *A*, HT29 cells were stimulated with 10 μg/ml anisomycin. For MK2/3 inhibition, cells were pretreated with 5 or 10 μM PHA-781089. p38 inhibitors BIRB-796 (1 μM) and SB202190 (5 μM) were used as positive controls. Phosphorylation of K20-Ser^{13}, K18-Ser^{52}, K8-Ser^{73}, and hHSPB1-Ser^{82} were analyzed by Western blotting. Total K20, K8/18, hHSPB1, and GAPDH were blotted to show equal loading. *B*, HT29 cells were stimulated with anisomycin (as in Fig. 1*B*) with or without treatment with 20 μM PHA-781089/5 μM SB202190. After treatment cells were fixed and double immunostained for K20 and K20-Ser(P)^{13}.

phorylation as that for mHSPB1 phosphorylation (Fig. 6*A*). Immunofluorescence staining of HT29 cells also showed reduced K20 phosphorylation in MK2 down-regulated cells (Fig. 6*B*). This supports the notion that K20 is a physiological substrate of MK2, similar to HSPB1. For all four different shRNAs tested, we could demonstrate perfect correlation between MK2 levels and K20-Ser^{13}/hHSPB1-Ser^{82} phosphorylation (supplemental Fig. 2).

K20 Phosphorylation Is Abrogated in MK2/3-deficient Mice—In the murine system, small intestine shows maximum expression of K20. K20-Ser^{13} phosphorylation was shown to be a stress marker especially in small intestinal goblet cells (18). Therefore, we analyzed K20-Ser^{13} phosphorylation in lysates of the ileum of MK2/3-deficient mice. K20-Ser^{13} phosphorylation was strongly reduced in the knockout compared with wild-type (WT) controls (Fig. 7*A*). This clearly shows that MK2/3 are protein kinases responsible for phosphorylation of K20 *in vivo*.

It was clearly shown previously that K20 is predominantly phosphorylated in small intestinal goblet cells (18), suggesting a role in goblet cell function. Immunostaining for K20-Ser^{13} phosphorylation in the ileum of MK2/3-double deficient mice compared with that of WT mice showed reduced staining in the lower two-thirds of the villi, a region that harbors the majority of the goblet cells (Fig. 7*B*). This finding supports the notion that MK2/3 are the main protein kinases responsible for K20-Ser^{13} phosphorylation in mucin-secreting goblet cells.

Pharmacological Blockade of p38 or MK2/3 Inhibits PGE2-stimulated Mucin Secretion—Early studies have shown the presence of an intermediate filament-containing barrier in close proximity to mucin storage granules (28). K20 phosphorylation was shown to be a small intestinal goblet cell marker (18), and K8-deficient mice are characterized by the presence of enlarged goblet cells (29). Therefore, we analyzed a possible role for p38/MK2/3-mediated K8/K20 phosphorylation in the

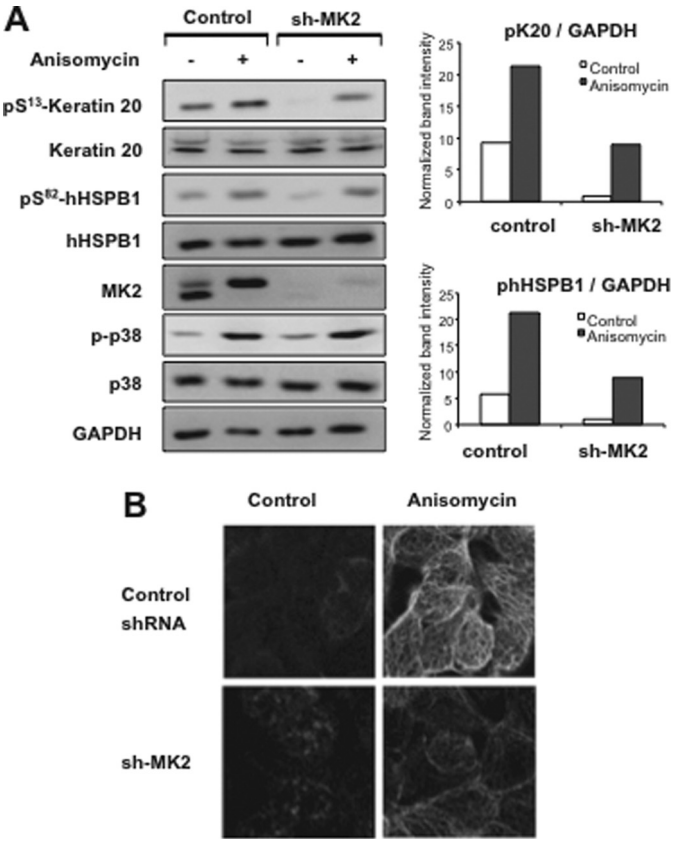

FIGURE 6. **Specific knockdown of MK2 reduces stress-induced K20 phosphorylation.** *A*, control shRNA or MK2 shRNA-transduced and selected HT29 cells were treated with 10 μg/ml anisomycin for 30 min. Lysates were analyzed by Western blotting using the indicated antibodies. Band intensities for pK20 and pHSPB1 were normalized to that of GAPDH to account for loading differences and plotted. *B*, control and MK2 shRNA-transduced HT29 cells were stimulated with anisomycin for 30 min or left untreated and then stained for K20-Ser(P)[13].

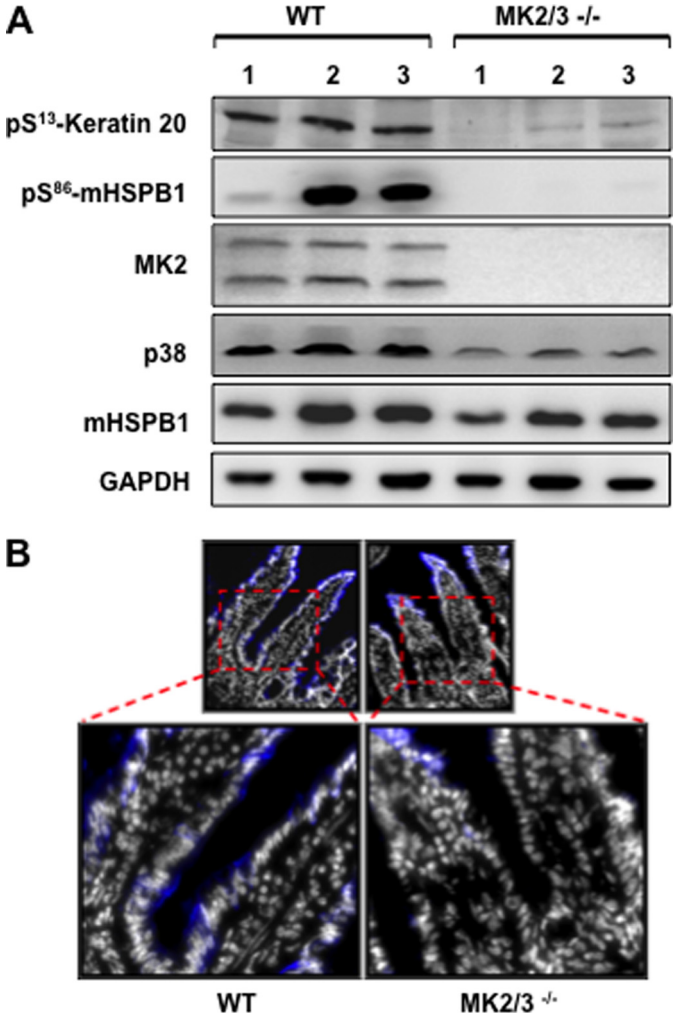

FIGURE 7. **Keratin 20 phosphorylation is abrogated in MK2/3$^{-/-}$ mice ileum.** *A*, ileum tissue from three WT and MK2/3-double deficient mice each were processed as mentioned under "Materials and Methods" and subjected to Western blotting using the indicated antibodies. *B*, small intestinal villi from WT and MK2/3$^{-/-}$ mice stained for K20-Ser[13] (*blue*) and nuclei (*white*) show reduced levels of phosphorylation at the base of villi (see *insets*).

process of mucin exocytosis. Because prostaglandins are physiologically relevant stimuli for intestinal cells, we analyzed PGE2-induced mucin secretion in HT29-MTX cells. The kinetics of PGE2-induced mucin secretion correlates well with the phosphorylation of K20 (Fig. 8, *A* and *B*). Both processes peaked at about 20 min and were sensitive to SB202190. Mucin amounts in the supernatants declined after 20–30 min probably due to gel formation and insolubilization. p38 inhibitors as well as the MK2/3 inhibitor PHA-781089 significantly blocked PGE2-induced mucin secretion from HT29-MTX cells (Fig. 8*C*). Because the inhibitor studies in differentiated intestinal epithelial cells demonstrated a p38- and MK2-dependent mucin secretion in response to PGE2, we also compared intestinal mucin secretion between MK2/3 DKO and WT mice using a modified ELLA integrated with *in vivo* ileal loop experiment (24) (Fig. 8*D*). In this experiment the PGE2-stimulated mucin secretion peaked at 10 min, consistent with a recent report (30). However, MK2/3 DKO mice did not show any statistically significant reduction in overall PGE2-induced mucin secretion compared with WT mice, probably because the intestinal villi contain multiple PGE2-responsive mucin-secreting cell types that interfere with the goblet cell-specific response.

DISCUSSION

Intermediate filament proteins including keratins show several features of stress response proteins including stress-induced up-regulation and phosphorylation (31). The data presented in this study suggest a dual role for the p38 pathway in keratin filament regulation, where p38 phosphorylates the type II keratins (for example K8-Ser[73]) and MK2/3 phosphorylate the type I keratins (K18-Ser[52], K20-Ser[13]) (*cf.* Figs. 7 and 9). In our study, phosphorylation of K19-Ser[35] (23) was not analyzed due to lack of phospho-specific antibodies. However, it is interesting to note that K19-Ser[35] is also located within an R*XX*S motif and shows similarity to K18-Ser[52] in several aspects (32). In addition, K8/19 were shown to become tyrosine-phosphorylated upon pervanadate stimulation in a p38-dependent manner (33), which increases complexity of p38 signaling to keratins. It is also significant that all p38/MK2-dependent phosphorylations we identified contribute significantly to stress-dependent and cell cycle-dependent reorganization of the keratin cytoskeleton (5, 14, 18, 34).

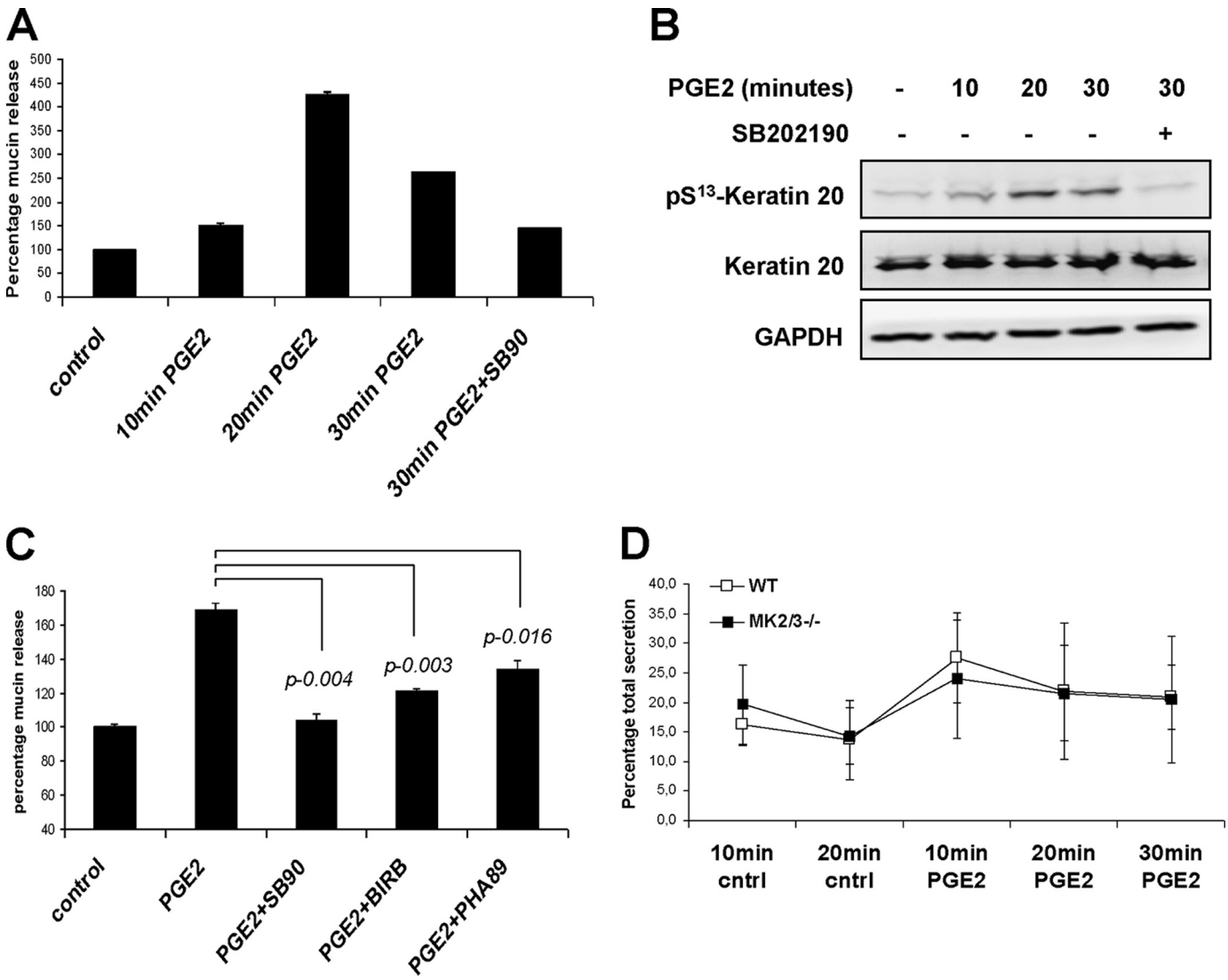

FIGURE 8. **K20 phosphorylation in PGE2-induced mucin secretion.** *A*, differentiated HT29-MTX cells were stimulated with 5 μM dimethyl-PGE2 for indicated times, and mucin-like glycoproteins in the supernatants were quantified by ELLA as described under "Materials and Methods." Where indicated, the cells were pretreated with 5 μM SB202190 for 30 min. *B*, cell lysates from the same experiment were probed with pK20 antibodies. Total K20 and GAPDH are shown as loading controls. *C*, mucin-like glycoprotein secretion was measured in HT29-MTX culture supernatants. Cells were left untreated or were treated with dimethyl-PGE2 (1 μM) for 30 min to allow mucin exocytosis. To study the role of p38-MK2 pathway, cells were pretreated for 30 min with 5 μM SB202190 (*SB90*), 1 μM BIRB-796 (*BIRB*), or 25 μM PHA-781089 (*PHA89*). *D*, mucin-like glycoprotein content was measured in small intestinal (ileum) effluents before (10 and 20 min) and after dimethyl-PGE2 stimulation (5 μM) (10, 20, and 30 min). The total mucin secreted in the entire assay duration (50 min) was taken as 100%, and the percentage fractions of mucin secreted at each time interval were plotted. The figure shows mean ± S.D. (*error bars*) of seven mice of each genotype.

K8/18 hyperphosphorylation correlates with disease progression in patients with chronic liver disease (35). Transgenic mouse overexpressing the human liver disease-associated K8-G61C variant showed reduced K8 phosphorylation and increased susceptibility to liver injury. K8-S73A transgenic mice showed a similar phenotype. This suggested K8-Ser^{73} to act as a phosphate sponge, thus protecting hepatocytes from proapoptotic effects of stress-activated protein kinases (36). Even though the K18-Ser^{52} site is not conserved in the murine system, it was identified as the major K18 phosphorylation in human cells induced by heat stress, G_2/M phase cell cycle arrest, and okadaic acid treatment (16). Studies with K18-S52A transgenic mice showed that K18-Ser^{52} phosphorylation has a hepatoprotective function (37). This phenotype and our finding about the involvement of stress-activated p38/MK2 pathway in K18-Ser^{52} phosphorylation support the phosphate sponge hypothesis. Reduced phosphorylation of MSK1 and HSPB1 in keratin-transfected MEFs (Fig. 4), compared with nontransfected cells, also suggests a role for keratins in dampening stress-activated protein kinase responses. Validation of this model would require analysis of human K18-WT and K18-S52A transgenic mice in combination with the MK2/3-deficient background.

p38/MK2/3 pathway plays a major role in innate immune defense via regulation of inflammatory cytokine biosynthesis (13). K20 phosphorylation in mucus-secreting cells in the intestine would suggest a more tissue-specific role for the pathway in innate immunity by regulating epithelial barrier function. Although we could show that K20 phosphorylation is drastically reduced in the basal part of intestinal villi in the

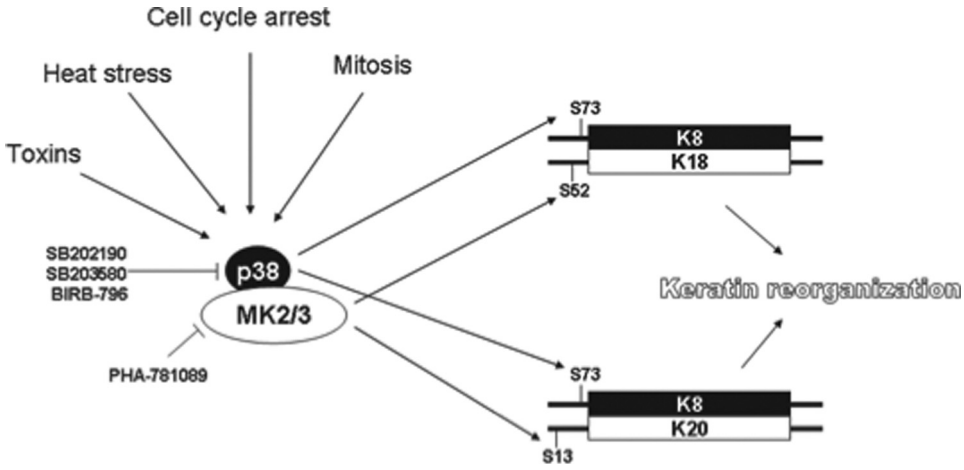

FIGURE 9. **Complex regulation of keratins by the p38 pathway.** p38/MK2/3 cooperation in keratin phosphorylation. p38 phosphorylates the type II keratin, K8 at Ser^{73}, whereas MK2 phosphorylates the binding partners K18 at Ser^{52} and K20 at Ser^{13}.

MK2/3$^{-/-}$ mice, some unexpected staining in the tip of the villi did not correlate with the Western blot results. This probably results from some cross-reaction of the antibodies in immunohistochemistry. In a goblet cell culture model (HT29-MTX), PGE2-stimulated mucin release correlated well with K20 phosphorylation and showed a clear dependence on activity of p38 as well as MK2. This is a stimulus- and cell type-specific effect because phorbol 12-myristate 13-acetate, a strong activator of PKC-induced mucin secretion, is independent of p38 activation (supplemental Fig. 3) and because other cells of the ileum could compensate the lack in mucin secretion (Fig. 8*D*). Therefore, it is proposed that the p38/MK2/3-dependent K20 phosphorylation contributes to mucin secretion in goblet cells.

Although the p38/MK2 pathway is considered to be proinflammatory, inflammatory bowel disease-like intestinal pathology in mice lacking the AU-rich element of TNF mRNA (TNF$^{\Delta ARE}$) was exacerbated in the absence of MK2, showing an antiinflammatory role in the intestine at least in this genetic model (38). The dextran sodium sulfate-induced colitis model and worm infection model of colitis showed no significant differences related to MK2/3 deficiency.[3] It would be interesting to study whether p38/MK2 has any role in a small intestinal inflammation model. It is important to note that K8-null mice develop spontaneous colitis (39, 40) associated with mistargeting of ion transporters and enlargement of goblet cells (29). However, intestinal bicarbonate secretion was not affected in MK2/3-deficient mice (data not shown). Preliminary experiments showed enhanced basal fluid uptake in the MK2/3 small intestine, but statistical evaluation needs more experiments.[4] Hence, further studies are required to understand the complete role of K8/K20 phosphorylation in fluid uptake and epithelial permeability/barrier function in MK2/3-deficient intestine.

A role for p38 in K8 phosphorylation is well documented (5, 6), which could be extended to other type II keratins with a conserved site homologous to K8-Ser^{73} (21). On the other hand, protein kinase C, casein kinases, and protein kinase A were suggested as physiological kinases involved in type I keratin phosphorylation. For example, another potential physiological kinase for K20-Ser^{13} is calcium-independent protein kinase C (16).

In conclusion, we show herein that MK2/3 downstream from p38 is directly involved in K18-Ser^{52} and K20-Ser^{13} phosphorylation. Because MK2/3-deficient mice are also characterized by reduced p38 levels and activity (13), they are severely compromised in stress-induced keratin phosphorylation. Further studies in this genetic model could thus be helpful in better understanding the physiological role of co-ordinated K8/18/20 phosphorylation under stress conditions.

Acknowledgments—We thank Dr. Qin Zhou (Stanford) for helpful discussion, Tatiana Yakovleva (Hannover) for help with mice breeding and genotyping, Michaela Friedrichsen (Hannover) for help with immunohistochemistry, Dr. Harald Herrmann (German Cancer Research Center-DKFZ) for providing antibodies against recombinant K8/K18 and K8, Dr. Thecla Lesuffleur (INSERM UMR S938, France) for providing HT29-MTX cells, and Dr. Robert J. Mourey (Pfizer Global R&D) for the gift of PHA-781089. M. B. M. thanks the Ph.D. program "Molecular Medicine" of the Hannover Medical School.

[3] M. B. Menon, A. Kotlyarov, and O. Pabst, unpublished data.
[4] A. Kumar Singh and M. B. Menon, unpublished data.

REFERENCES

1. Schweizer, J., Bowden, P. E., Coulombe, P. A., Langbein, L., Lane, E. B., Magin, T. M., Maltais, L., Omary, M. B., Parry, D. A., Rogers, M. A., and Wright, M. W. (2006) *J. Cell Biol.* **174,** 169–174
2. Omary, M. B., Ku, N. O., Strnad, P., and Hanada, S. (2009) *J. Clin. Invest.* **119,** 1794–1805
3. Omary, M. B., Ku, N. O., Tao, G. Z., Toivola, D. M., and Liao, J. (2006) *Trends Biochem. Sci.* **31,** 383–394
4. Roux, P. P., and Blenis, J. (2004) *Microbiol. Mol. Biol. Rev.* **68,** 320–344
5. Ku, N. O., Azhar, S., and Omary, M. B. (2002) *J. Biol. Chem.* **277,** 10775–10782
6. Wöll, S., Windoffer, R., and Leube, R. E. (2007) *J. Cell Biol.* **177,** 795–807
7. Gaestel, M. (2006) *Nat. Rev. Mol. Cell Biol.* **7,** 120–130
8. Rousseau, S., Dolado, I., Beardmore, V., Shpiro, N., Marquez, R., Nebreda, A. R., Arthur, J. S., Case, L. M., Tessier-Lavigne, M., Gaestel, M., Cuenda, A., and Cohen, P. (2006) *Cell. Signal.* **18,** 1897–1905
9. Kotlyarov, A., Yannoni, Y., Fritz, S., Laass, K., Telliez, J. B., Pitman, D., Lin, L. L., and Gaestel, M. (2002) *Mol. Cell. Biol.* **22,** 4827–4835
10. Menon, M. B., Ronkina, N., Schwermann, J., Kotlyarov, A., and Gaestel, M. (2009) *Cell Motil. Cytoskeleton* **66,** 1041–1047
11. Cheng, T. J., and Lai, Y. K. (1998) *J. Cell. Biochem.* **71,** 169–181
12. Kasahara, K., Kartasova, T., Ren, X. Q., Ikuta, T., Chida, K., and Kuroki, T. (1993) *J. Biol. Chem.* **268,** 23531–23537
13. Ronkina, N., Kotlyarov, A., Dittrich-Breiholz, O., Kracht, M., Hitti, E., Milarski, K., Askew, R., Marusic, S., Lin, L. L., Gaestel, M., and Telliez, J. B. (2007) *Mol. Cell. Biol.* **27,** 170–181
14. Liao, J., Ku, N. O., and Omary, M. B. (1997) *J. Biol. Chem.* **272,** 17565–17573
15. Ku, N. O., and Omary, M. B. (1997) *J. Biol. Chem.* **272,** 7556–7564

16. Liao, J., Lowthert, L. A., Ku, N. O., Fernandez, R., and Omary, M. B. (1995) *J. Cell Biol.* **131,** 1291–1301
17. Ku, N. O., Liao, J., and Omary, M. B. (1998) *EMBO J.* **17,** 1892–1906
18. Zhou, Q., Cadrin, M., Herrmann, H., Chen, C. H., Chalkley, R. J., Burlingame, A. L., and Omary, M. B. (2006) *J. Biol. Chem.* **281,** 16453–16461
19. Ku, N. O., and Omary, M. B. (2000) *J. Cell Biol.* **149,** 547–552
20. Chou, C. F., and Omary, M. B. (1993) *J. Biol. Chem.* **268,** 4465–4472
21. Lesuffleur, T., Porchet, N., Aubert, J. P., Swallow, D., Gum, J. R., Kim, Y. S., Real, F. X., and Zweibaum, A. (1993) *J. Cell Sci.* **106,** 771–783
22. Barjaktaroviæ, Z., Schütz, W., Madlung, J., Fladerer, C., Nordheim, A., and Hampp, R. (2009) *J. Exp. Bot.* **60,** 779–789
23. Engel, K., Schultz, H., Martin, F., Kotlyarov, A., Plath, K., Hahn, M., Heinemann, U., and Gaestel, M. (1995) *J. Biol. Chem.* **270,** 27213–27221
24. Singh, A. K., Riederer, B., Chen, M., Xiao, F., Krabbenhoft, A., Engelhardt, R., Nylander, O., Soleimani, M., and Seidler, U. (2010) *Am. J. Physiol. Cell Physiol.* **298,** C1057–C1065
25. Trompette, A., Blanchard, C., Zoghbi, S., Bara, J., Claustre, J., Jourdan, G., Chayvialle, J. A., and Plaisancé, P. (2004) *Eur. J. Cell Biol.* **83,** 347–358
26. He, T., Stepulak, A., Holmström, T. H., Omary, M. B., and Eriksson, J. E. (2002) *J. Biol. Chem.* **277,** 10767–10774
27. Toivola, D. M., Zhou, Q., English, L. S., and Omary, M. B. (2002) *Mol. Biol. Cell* **13,** 1857–1870
28. Specian, R. D., and Oliver, M. G. (1991) *Am. J. Physiol. Cell Physiol.* **260,** C183–C193
29. Toivola, D. M., Krishnan, S., Binder, H. J., Singh, S. K., and Omary, M. B. (2004) *J. Cell Biol.* **164,** 911–921
30. Garcia, M. A., Yang, N., and Quinton, P. M. (2009) *J. Clin. Invest.* **119,** 2613–2622
31. Toivola, D. M., Strnad, P., Habtezion, A., and Omary, M. B. (2010) *Trends Cell Biol.* **20,** 79–91
32. Zhou, X., Liao, J., Hu, L., Feng, L., and Omary, M. B. (1999) *J. Biol. Chem.* **274,** 12861–12866
33. Feng, L., Zhou, X., Liao, J., and Omary, M. B. (1999) *J. Cell Sci.* **112,** 2081–2090
34. Ku, N. O., and Omary, M. B. (1994) *J. Cell Biol.* **127,** 161–171
35. Toivola, D. M., Ku, N. O., Resurreccion, E. Z., Nelson, D. R., Wright, T. L., and Omary, M. B. (2004) *Hepatology* **40,** 459–466
36. Ku, N. O., and Omary, M. B. (2006) *J. Cell Biol.* **174,** 115–125
37. Ku, N. O., Michie, S. A., Soetikno, R. M., Resurreccion, E. Z., Broome, R. L., and Omary, M. B. (1998) *J. Cell Biol.* **143,** 2023–2032
38. Kontoyiannis, D., Boulougouris, G., Manoloukos, M., Armaka, M., Apostolaki, M., Pizarro, T., Kotlyarov, A., Forster, I., Flavell, R., Gaestel, M., Tsichlis, P., Cominelli, F., and Kollias, G. (2002) *J. Exp. Med.* **196,** 1563–1574
39. Habtezion, A., Toivola, D. M., Butcher, E. C., and Omary, M. B. (2005) *J. Cell Sci.* **118,** 1971–1980
40. Baribault, H., Penner, J., Iozzo, R. V., and Wilson-Heiner, M. (1994) *Genes Dev.* **8,** 2964–2973